Electromagnetic Noise Contamination on Transient Electromagnetic Soundings in Culturally Disturbed Environments

Mette S. Munkholm[1] and Esben Auken[2]

University of Aarhus, Department of Earth Sciences[1] and
Technical University of Denmark, Department of Geology and Geotechnical Engineering[2] (formerly at 1)

ABSTRACT

Knowledge of the noise level and the nature of the noise is critical when processing transient electromagnetic (TEM) sounding data. An inadequate noise estimation may result in an erroneous interpretation. We consider the sources of electromagnetic noise and their influence on TEM soundings. The focus is on the characteristics of the vertical component of the noise for an impulse response system which measures log-gated, gated stacked voltages, induced from a decaying secondary field. A fully automatic, hands-off algorithm for calculation of a noise model is developed and replaces the previous manual and subjective weeding out of poor data which was based on the experience of the interpreter. The method enables an assignment of uncertainty to each delay time data giving a more correct and hence more reliable use of the measurements at late times. The algorithm is developed through a comparison of noise characteristics for simulated white, Gaussian noise and EM noise measurements sampled every 2 μsec. It is tested on data obtained with a receiver which implements the log-gating, gate stacking measurement scheme. This automatic noise estimation has been used in the inversion of well over 4000 TEM soundings. Noise weighted data are inverted and the resulting changes in model parameters are discussed for an example with model data and real noise and a field example. The model from the field data is correlated with a drilling.

Introduction

The transient electromagnetic, TEM, method has been used extensively in the search for mineral deposits and metallic ores (Buselli et al., 1986; Staples, 1984). Within the past decade the method has gained increased recognition in hydrogeological and environmental surveys. Examples of case studies are presented in Mills et al. (1988) and Goldman et al. (1991) in which TEM data map the seawater intrusion in coastal regions in California and Israel, respectively. In Auken et al. (1994) TEM data in combination with other geophysical data are used to determine the volumetric extent of an aquifer. Both in mining and in hydrogeophysics investigations it is the ability of the TEM method to resolve the depth to a good conductor that is being exploited.

With the growing need for good quality groundwater, the demand for hydrogeophysical surveys to determine the extent, the quality and the vulnerability of aquifers is bound to increase. To ensure the water supply to both small and large cities the survey area will in many cases lie in densely habited areas full of pipes and power lines, both above and below the surface. In such culturally disturbed areas electromagnetic noise arising from cultural sources is superposed on the noise from natural sources, resulting in an increased noise level and a much poorer data quality than in more remote locations.

As increasing delay time corresponds to increasing penetration depth, the depth of penetration for a TEM sounding in principle depends on the latest delay time measured. In practice though, the latest useful delay time is limited by the EM noise level at the sounding site (Spies, 1989). Naturally, increasing the transmitter moment increases the signal level. However, in groundwater surveys fairly small, mobile systems with transmitter moments on the order of 5000 Am^2 are generally used.

We wish to construct a scheme in which data are automatically weighted in accordance with the noise level at a given delay time. Based on the decrease in signal to noise ratio with delay time a sounding curve may be divided into three intervals as shown in fig. 1. At early delay times the data quality is superb and the data should be kept without doubt. At late delay times, when the signal has been overwhelmed by noise, the data quality is so poor that the data may be disregarded. At intermediate times the data quality is not as good as in the first interval. On the other hand the signal has not yet been overwhelmed by noise. The question therefore arises how to weight the data in the transition zone. Interpretation of either only the low noise data or the low noise and the transition data is suboptimal. The objective of this paper is to devise an automatic procedure for noise estimation with more correct and hence reliable assignment of error bars to the measurements in the transition interval.

We study EM noise in relation to TEM receiver systems which operate by log-gating and gate stacking data. For data obtained with such a system it is not possible to carry out

an analysis of the frequency content and statistical characteristics of EM noise. We manage to evade the problem by studying the noise characteristics for equidistant sampled EM noise and modify the results to log-gated, gate stacked data. A noise model is presented based on numerical simulations of log-gating and gate stacking on synthetic, white, Gaussian noise and on actually measured EM noise time series. It is based on a generalization of the decrease of the standard deviation of Gaussian distributed data with stack size. As the time series show that the EM noise is colored and that outliers occur occasionally, it is necessary to study the effects on the noise model of the deviation from the assumptions of whiteness and Gaussianity for real noise. Therefore, noise model calculations for these data are compared with the calculations for the synthetic data. We investigate the model extraction ability with and without the noise model and finally the noise model is used on field data measured with a log-gating, gate stacking receiver. The differences that can occur between interpretations with and without use of the noise model are thereby illustrated.

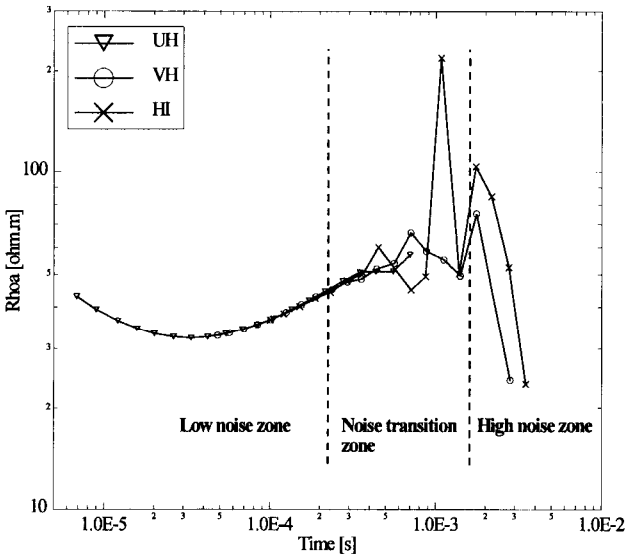

Figure 1. A typical transient electromagnetic sounding curve measuring the decay of the vertical magnetic field in the central loop configuration. The field values have been converted to late time apparent resistivity. The sounding has been measured in three partly overlapping time intervals: early delay times (UH), intermediate delay times (VH) and late delay times (HI). The markers on the curves show the data points. At early times the signal to noise ratio is superb whereas at late times the signal is lost in noise. At intermediate times, in the noise transition zone, the data are partly disturbed by the noise. The border between the low noise zone and the noise transition zone is in this case at about 0.21 ms and is drawn where the sounding curves begin to diverge. The border to the high noise zone, although more difficult to define, is drawn at 1.6 ms.

The Electromagnetic Noise Spectrum

The EM noise can be divided into two major types, namely arising from natural sources and from cultural sources. The noise spectrum has daily, annual and geographic variations. In the following a brief review of the sources is given and a more thorough discussion of the EM noise spectrum may be found in e.g. Macnae et al. (1984), McCracken et al. (1986) and Spies & Frischkneckt (1991).

For natural sources the EM noise below 1 Hz arises mainly from an interaction between the earth's magnetic field and plasma emitted from the sun. Of more interest in TEM soundings is the spectrum above 1 Hz. The major contributor above 1 Hz is lightning discharges from thunderstorms. Distant thunderstorm activity produces a background noise level whereas strong sferics arise from nearby or intermediate distances. The fields travel in the Earth-ionosphere cavity. Sferics occur worldwide at a frequency of approximately 100 per second.

In populated areas cultural sources contribute to the noise as well, thereby increasing the noise level. In culturally disturbed areas the power distribution grid is one of the main noise contributors, resulting in spectral peaks at 50 or 60 Hz and at their odd harmonics. Although the voltage waveform is kept sinusoidal at 50 or 60 Hz the current producing disturbing fields fluctuates from sinusoidal waveform due to the varying load on the grid and high amplitude, broadband transients occur occasionally. Furthermore, spectral peaks due to VLF transmitters and other radio transmitters around the globe are significant noise contributors.

Source generated noise arises from cultural conductors such as buried pipelines and cables in the vicinity of the sounding and can be major noise contributors (Nekut and Eaton, 1990). Currents are induced in the conductors from power lines and communication transmitters. These induced currents give rise to a secondary field coherent with the earth response and the two signals will be superposed.

Suppression of EM Noise

In contrast to frequency domain systems time domain EM systems are inherently broadband. In frequency domain systems bandpass filters are employed to reject frequencies other than the signal frequency. As shown in Macnae et al. (1984) a time domain EM system which uses some form of synchronous averaging has a spectral response collapsed to that of a multitude of narrow spectral lines, centered on the odd harmonics of the basic repetition frequency. It rejects incoherent noise with a stationary statistical character, whereas the earth's response is emphasized since it is in phase with the basic repetition frequency.

It is more difficult to suppress the noise from the power distribution grid and from sudden strong transients. The only way to reject coherent noise is to shift the repetition frequency

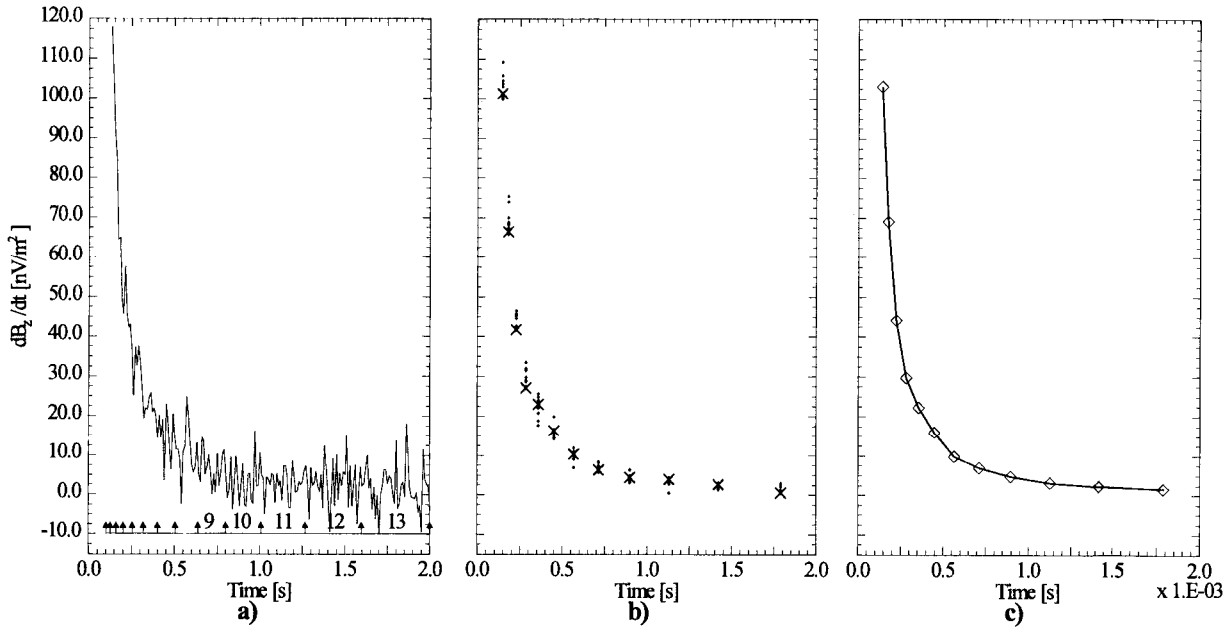

Figure 2. a) A transient electromagnetic response has been generated over a 1D 2-layered earth model in the time interval from 0.1 ms to 2 ms. The response is sampled with a sampling frequency of 100 kHz. Gaussian noise with zero mean and a standard deviation of 5 nV/m^2 has been added to the transient decay. The logarithmically spaced time windows are shown at the bottom of the plot - only the last five time windows are numbered. b) The log-gated transient decay of the noise-contaminated response shown in a) are marked with a x. The • represents nine other noise contaminated log-gated transient responses. c) The gated stacked response of the ten log-gated responses from b). The data points are marked with a ◊.

away from the frequency of that noise, e.g. away from the power network frequency. Strong sferics and power line transients occasionally result in instability of receiver amplifiers for some time after the reception of the transient and may be critical for the signal to noise ratio as the gate values are sensitive to strong noise transients. Another problem is responses from buried pipelines and cables which are enhanced along with the earth's response through stacking.

Log-gating, Gate Stacking of EM Noise

Log-gating refers to an integration of the input over time intervals with lengths that increase logarithmically with delay time, whereas gate stacking refers to the subsequent stacking of all gates with the same delay time. A principal sketch of this is shown in fig. 2. A noise contaminated transient decay is shown in fig. 2a. The numbered intervals on the time axis indicate the time windows used in the gating. Notice that the axes in this plot are linear to emphasize the increase in window width with delay time. The earth response changes most rapidly at early delay times requiring a dense sampling to represent the changes whereas at later delay times the signal to noise ratio deteriorates requiring longer averaging intervals to extract the earth response (Nabighian and Macnae, 1991). One way of implementing this is as windows equidistantly spaced in logarithmic time. The term log-gating refers to the calculation of a mean value within each of these logarithmically spaced time windows, to represent the decay at the center time of that window (fig. 2b). Repeated measurements of the earth response are log-gated and subsequently the values at the same delay time are stacked (fig. 2c). The latter process is referred to as gate stacking. In practice often 1000 or more log-gated transients need to be gate stacked to obtain the desired signal to noise ratio.

For white, Gaussian noise an increase in stack size by a factor N will result in a decrease in the standard deviation of the noise by a factor $\sqrt{N}$. Due to the increase in integration time with increasing delay times the effect of log-gating is to increase the stack size for progressively later time gates and thereby obtain a decrease in the standard deviation of the noise with time by a factor of the square root of the gate length. Equation 1 states that the mean of the absolute value of zero-mean Gaussian distributed data |x| is proportional to the standard deviation, σ,

$$E|x| = \frac{1}{\sqrt{2\pi\sigma}} \int_{-\infty}^{\infty} |x| \exp(-\frac{x^2}{2\sigma^2})dx$$

$$\Updownarrow$$

$$E|x| = \frac{2\sigma}{\sqrt{2\pi}} \qquad (1)$$

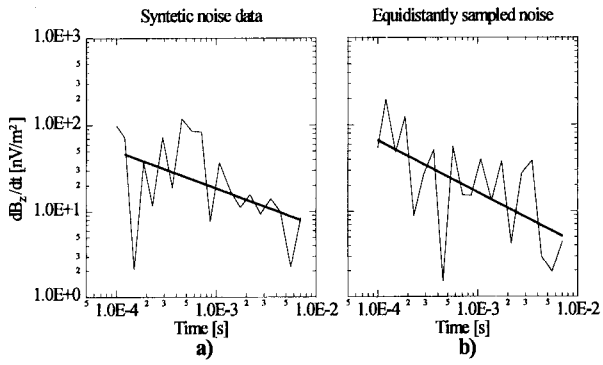

Figure 3. a) The result of log-gating and gate stacking 1124 synthetic Gaussian noise series each with zero mean and a standard deviation of 10^4 nV/m² and sampled every 2 μsec. The noise model shown as the solid straight line has a slope of -0.49 and an intercept of 0.3 nV/m². b) The result of log-gating and gate stacking 1124 real noise series measured with a sampling density of 2 μsec. The slope of the noise model is -0.60 and the intercept is 17 nV/m².

It follows that the absolute value of log-gated, gate stacked Gaussian noise is expected to plot as a line with a slope of -½ in a log-log plot.

In the following a noise model given as a linear least squares fit in log-log space to the absolute values of log-gated, gate stacked noise is investigated. The noise model has the form

$$dB_z/dt = bt^a \qquad (2)$$

where b is a constant of proportionality, t is time and a is the slope. For log-gated, gated stacked Gaussian noise a=-½.

The late stage behavior of a transient response over a layered halfspace is that of an equivalent homogeneous halfspace with the resistivity of the lower layer. For an impulse response system the late stage decay is proportional to $t^{-5/2}$. Assuming that the sounding curve has reached the late stage and comparing with the $t^{-1/2}$ proportionality of the noise model, the transition between data with a high and a low S/N ratio is rather abrupt. Fitterman (1989) determines the latest time of measurable signal for a given noise level using typical levels rather than noise measured at the sounding site. Extrapolating this noise level to the entire delay time range would result in an even more abrupt transition between data with a high and low S/N.

Simulated White, Gaussian Noise

Synthetic Gaussian noise series with zero mean sampled every 2 μsec in the interval from 0.1 ms to 7 ms are shown after log-gating and gate stacking in fig. 3a. The level on the synthetic noise is chosen based on observed standard deviations of 10^4 nV/m² for measured EM noise series sampled with the same density. The resulting noise model for the series shown in fig. 3a has a slope of -0.43 and an intercept at 1 ms of 18 nV/m². The average slope for 20 simulations is -0.54 with the standard deviation 0.16.

Equidistantly Sampled Noise

The data presented in this section are real measurements of the electromagnetic noise in an urban, culturally disturbed area of Denmark. The vertical component of the EM noise has been measured with a receiver which samples data every 2 μsec, in the interval from 2 μsec to 8 ms. A section of length 1 ms is shown in fig. 4a. The standard deviation of this noise series is 15.000 nV/m². In this example we hardly observe any outlier noise bursts. Gaussianity is tested by X^2-tests (Press et al., 1992) rendering 73% out of 200 series Gaussian at a significance level above 0.68 (see fig. 5).

The amplitude spectral density shown in fig. 4b shows that up to 250 kHz the noise is not white. Two of the more prominent spectral lines at 15.1 kHz and at 244.1 kHz coincide with the transmitting frequency of a VLF transmitter in Bordeaux, France and a longwave radiotransmitter in Denmark, respectively.

In the previous section we tested the noise model on simulated white Gaussian data. From the real measurements of the EM noise we observed that the noise for a high percentage of the series is Gaussian at a high significance level, but that the noise is not white but colored. The effect of this on the noise model is investigated by log-gating and gate stacking the equidistantly sampled noise series. It is carried out on a stack of 1124 real noise series, each at a length of 8 ms. An example of a noise model fitted to the log-gated, gate stacked real noise is shown in fig. 3b. The resulting noise model has a slope of -0.60 and an intercept at 1 ms of 17 nV/m². Similar noise measurements have been carried out in three different locations and result in an average slope of -0.71. The standard deviation for these slopes is 0.11.

Log-Gated, Gate Stacked Measured Noise

The commercially available PROTEM receiver (Geonics LTD.) implements the log-gating, gate stacking measurement technique. Noise measurements with the PROTEM receiver have been carried out at seven test sites to compare the slopes of the resulting noise models under different noise conditions. 30-45 log-gated, gate stacked noise series were measured at each of the test sites. A noise measurement is carried out by measuring the field with the receiver without transmitter emission. Depending on the geology and the noise level, the PROTEM receiver may measure the transient decay for up to three segments, covering the delay time interval from 6.85 μsec to 7.04 ms.

The example presented here consists of soundings measured for all three time segments, along with 25 noise measurements for the first segment, 10 for the second and 10 for

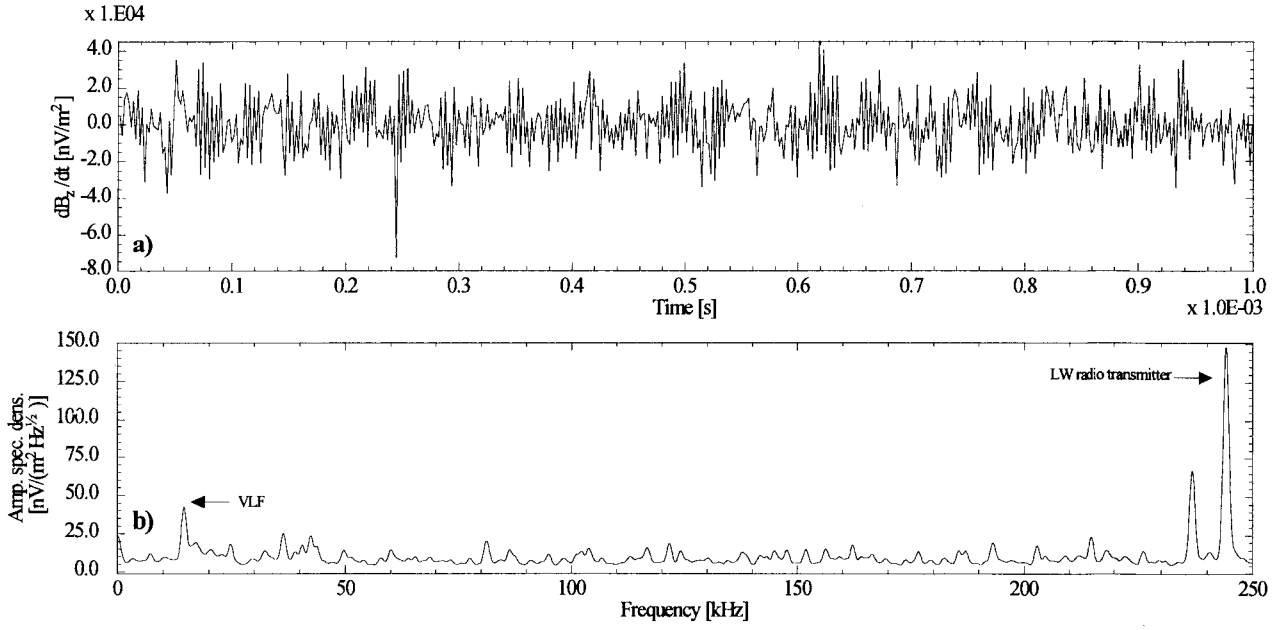

Figure 4. a) A 1 ms long section of an EM noise series with a sampling density of 2 μsec. The field oscillates but is generally contained within a band between -25000 nV/m² and 25000 nV/m². A few noise bursts occur, e.g. at 0.243 ms. b) Average amplitude spectral density up to 250 kHz for EM noise. Spectral lines are observed as for instance at 244.1 kHz, a Danish longwave radiotransmitter frequency, a factor 15 higher in amplitude than the general level at 10 nV/m²/Hz½.

the third segment (see fig. 6a). At a delay time of approximately 1 ms the sounding reaches the noise level at 6 nV/m² whereupon it is lost in noise. In fig. 6b a stack of the noise measurements for each segment is shown. The resulting noise model, based on the measurements on the third segment which contains the noise transition zone, has a slope of -0.43, slightly less steep than the -1/2 expected for Gaussian noise. For the different test sites we found a mean slope value of -0.57 and a standard deviation of 0.19 on these slopes. In this case the noise level at 1 ms is 3.8 nV/m². Usually it lies in the range between 1-10 nV/m² at 1 ms.

In summary, although the expected slope of log-gated, gate stacked Gaussian noise is -½, a substantial scatter is observed even for simulated data. Therefore the difference in slope in the synthetic noise example in fig. 3a and the example based on equidistant EM noise in fig. 3b is acceptable. As the first couple of time windows are very narrow and contain only one of the 2 μs samples, one extreme realization has a high influence on the gate value after log-gating and can distort the noise model. Note for instance the extreme third datapoint in fig. 3a. Due to scatter on the slopes, estimating both the intercept and the slope of the noise model is superior to fixing the slope to -½ and only estimating the intercept. The value and the scatter of the slope estimated for both the time series and the log-gated, gate stacked measured noise are in the same range as that found for the simulated data. We conclude that in spite of the non-Gaussianity and non-whiteness of the true EM noise, the noise model, although based on assumptions of Gaussianity and whiteness, describes the actual noise characteristic quite well.

Noise Model Fitted to Production Requirements

The field procedure for production includes three noise measurements around the noise transition zone. As these measurements for the PROTEM receiver coincide with measure-

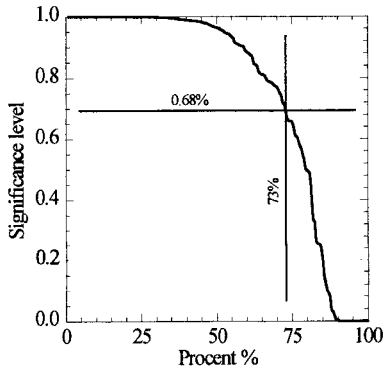

Figure 5. The significance of χ^2-tests for Gaussianity on 200 sets of noise measurements sampled at a sampling density of 2 μsec in the time interval 2 μsec to 8 ms. 73% of the series have significance levels above 0.68 (marked with the dashed lines). Thus, the test shows that 3/4's of these noise series are consistent with Gaussian distributions at a high significance level.

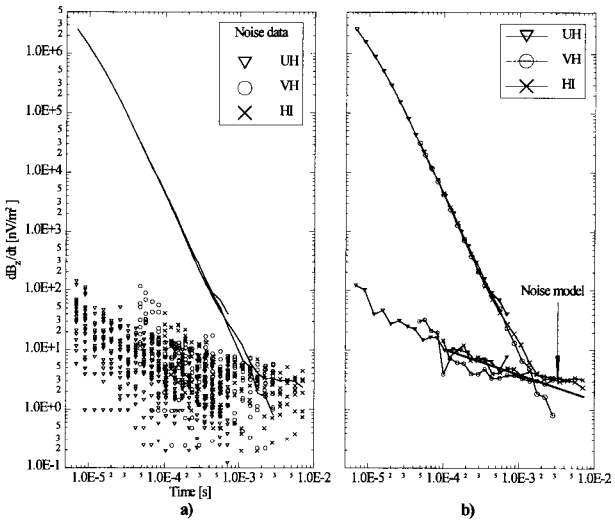

Figure 6. a) Three sounding segments measured with the PROTEM system along with 25 noise measurements on the first segment, 10 on the second and 10 on the third. Note the span of the noise data of more than three magnitudes at each delay time. The sounding is overwhelmed by noise at a delay time of 1 ms. b) The three sounding segments and the mean noise for each of the three segments. The noise model (solid straight line), based on the third segment which contains the noise transition zone, has a slope of -0.43 and an intercept of 3.8 nV/m².

ments needed to determine the noise saturation gain before performing a sounding, the measurement process does not become more time consuming. Initial noise models are determined as a least squares linear fit in log-log space to the absolute values of the individual measurements. However, outliers in the individual measurements will have a strong influence on the mean noise per gate and therefore some kind of outlier rejecting scheme should be used. We suggest disregarding values at a distance larger than 2σ of the initial noise model. Hereafter a mean noise per gate is calculated for the remaining data and a subsequent linear least squares log-log fit determines both the slope and the intercept of the final noise model in Eq. 2. The model is extrapolated to the entire time range of the sounding. Even though it is possible to estimate the noise model from any of the three segments the optimal estimate is found based on a segment in the noise transition zone. This is after all where the noise problem occurs.

A relative standard deviation, $\sigma_{noise,i}$, at each delay time is calculated as the ratio between the final noise model, given by Eq. 2, and the sounding data. Furthermore, geological complexity not accommodated by the 1-D earth model and transmitter-receiver misplacement contributes to the uncertainty of the data and must be included as a standard deviation, $\sigma_{o,i}$. In the Danish sedimentary geological environment $\sigma_{o,i}$ can typically be set to 3% - 5%. The standard deviation, σ_i, for delay time i is calculated as

$$\sigma_i = \sqrt{\sigma_{0,i}^2 + \sigma_{noise,i}^2} \qquad (3)$$

Time domain data are often presented as late time apparent resistivity data, ρ_a, given as

$$\rho_a(t) = \frac{\mu}{4\pi}\left(\frac{2\mu M}{5\,dB_z/dt}\right)^{\frac{2}{3}} t_c^{-\frac{5}{3}} \qquad (4)$$

where t_c are gate center times, dB_z/dt is the time derivative of the magnetic field, μ is $4\pi 10^{-7}$ H/m and M is the transmitter moment. Although the noise data contain no direct information on the conductivity structure of the earth the dB_z/dt noise can be converted into a pseudo-ρ_a noise. For this conversion the transmitter moment of the chosen extrapolation segment should be used. Substituting Eq. 2 into Eq. 4 results in

$$\rho_a(t) = \frac{\mu}{4\pi}\left(\frac{2\mu M}{5\,b}\right)^{\frac{2}{3}} t_c^{-\frac{5}{3}-\frac{2}{3}a} \qquad (5)$$

Thus, the noise model converted to apparent resistivity plots as a line with a slope of -1/3 (5+2a). For Gaussian data the slope is then -4/3.

Data Examples

To illustrate the practical implementation of the noise model two examples are presented. In the first example a sweep of different models, resulting from the inversion of a noise contaminated synthetic data set using different data cut off times, are compared with the model resulting from a noise weighted inversion using the noise model. The second example compares the noise weighted inversion results of a TEM sounding with results from a drill hole nearby.

Inversion of Noise Contaminated Synthetic Data

The sounding shown in fig. 1 is in fact model data to which real measured electromagnetic noise has been added. The sounding data are generated over a 1-D earth model (fig. 7b), with a first layer of 30 Ω•m and a thickness of 30 m, a second layer of 80 Ω•m and a thickness of 200 m and a lower halfspace with a resistivity of 10 Ω•m.

The average noise curve (fig. 7a) is the processed noise data based on three individual noise measurements on the segment containing the latest delay times. The noise model has a slope of approximately -0.44 (-1.4 in a ρ_a plot) and intercept of 2.5 nV/m² at 1.0 ms.

Before entering a 1-D inversion (Christensen and Auken, 1992) the data are ascribed a standard deviation of 3%. The standard deviation calculated from the noise model is added

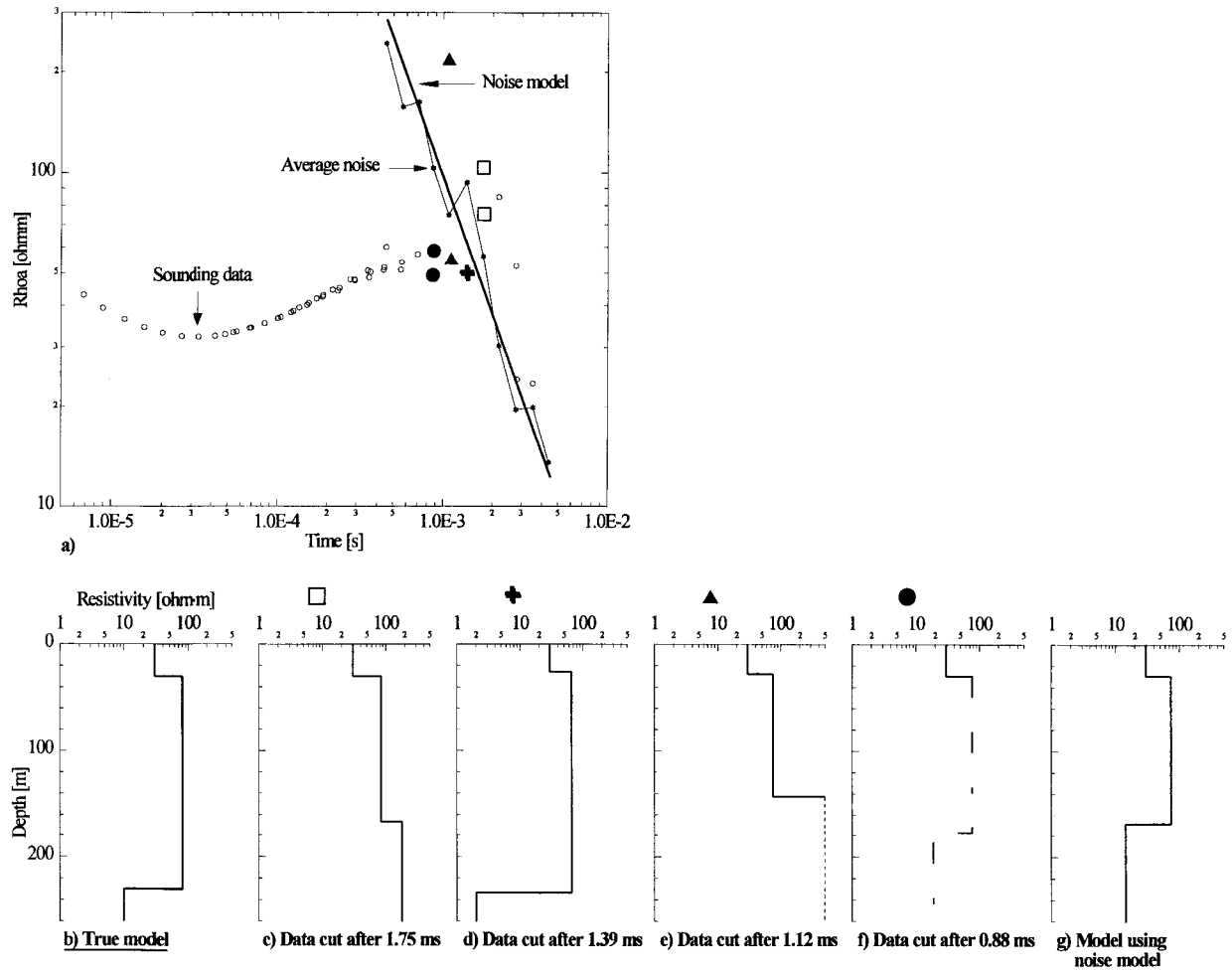

Figure 7. The sounding data, o, consists of a sum of synthetic data over the model shown on b) and measured EM noise. The average noise series, ✶, is for comparison converted into pseudo late time apparent resistivity. The cut off times at 0.88 ms (●), 1.12 ms (▲), 1.39 ms (+) and 1.75 ms ( ) are marked. At these delay times the intermediate (VH) and the late delay time (HI) segments overlap and therefore there are two data points per gate center time. c) - f) show the resulting models from the 1-D least squares inversions of the data set after weeding out data. The hatched line in e) indicates a resistivity exceeding 500 Ω•m. f) Hatched line indicating that a two layer model is adequate for the interpretation. g) Model resulting from an inversion using the noise model.

to these 3%. For early delay times with a high signal to noise ratio the standard deviation of the data remains approximately 3%, whereas at late delay times the standard deviation reaches 100% for data which have reached the noise line.

Alternatives to weighting of data according to the noise model, are either manually to weed out late delay time data with a jagged appearance, or to use the data for all delay times without regard to the noise level and the appearance of the data. Both cases are very dependent on the experience of the interpreter and can easily lead to misinterpretations. In the former case there is a risk of loosing or over-interpreting the information actually contained in the data about the resistivity structure of the ground. In the latter case the interpretation would partly be based on EM noise, appearing possibly in the interpretation as an extra non-geological layer. When the standard deviation is ascribed to the data based on in situ measured noise, it is less critical to be concerned about the validity of every single datum. Data with a large standard deviation are merely not weighted in the inversion scheme.

Figure 7 c-f show the ambiguity in the models obtained after a manual weeding out of noisy data. Different models are obtained for various data cut off time. Data at delay times later than the data cut off times have been removed from the data set, and to the remaining data a uniform standard deviation of 3% is ascribed.

In general the resistivity of the first two layers and the depth to the second layer are quite well retrieved as the information about these layers is contained at early times, where the signal to noise ratio is large. The depth to the third layer - if present at all - and the resistivity of the halfspace varies

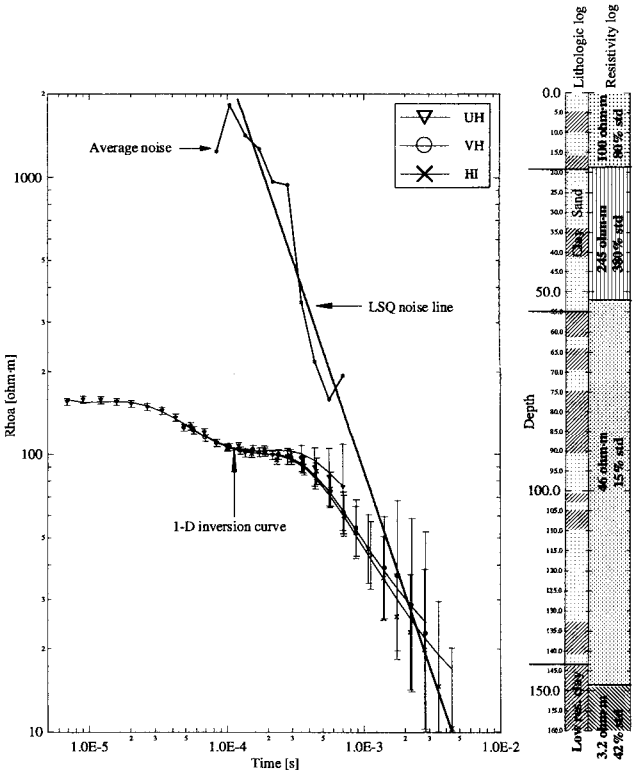

Figure 8. The sounding is performed in the central loop configuration with a moment of 4800 Am². The standard deviation increases from the obligatory 3% to approximately 100% at late delay times. The noise has been measured on the segment covering the early delay times (UH) and converted into a pseudo apparent resistivity noise curve. Only the last part of the noise curve is in the plot window. To the right is shown a resistivity log based on a four layer 1-D inversion of the time domain data along with a lithologic log from a drill hole at the same location. The lithologic log is divided into parts mainly consisting of sand and gravel (light dot pattern) and clay (hatched pattern). The resistivity of the clay is in the interval 2 Ω•m - 40 Ω•m and the resistivity of the sand ranges from 40 Ω•m to a couple of hundred Ω•m. On the resistivity log is shown the standard deviation (std) of the resistivities. Note how well the layer boundaries on the two logs agree.

with the data cut off time. Cutting the data at 1.75 ms results in a layer boundary at a depth of approximately 160 m and a halfspace resistivity of 200 Ω•m (fig. 7c) whereas cutting at 1.39 ms changes this to 240 m and 2 Ω•m (fig. 7d). When reducing the cut off time to 1.12 ms the boundary shows at a depth of 140 m and the resistivity exceeds 1500 Ω•m (fig. 7e). Finally the values obtained for these two model parameters when cutting the data at 0.88 ms are 180 m and 20 Ω•m, respectively (fig. 7f). With such an early cutting time a three layer interpretation is actually not feasible. The model parameters obtained are very uncertain and instead a two layer model interpretation should be attempted. Depending on the data cut off time, the depth varies roughly between a factor 0.6 and 1 of the true depth at 230 m, and the resistivity varies between a factor of 0.2 and a factor of more than 200 from the true 10 Ω•m.

The result of the inversion of the noise weighted data is shown in fig. 7g. All data have been used in the inversion. The depth to the halfspace is 170 m and the resistivity of the halfspace is 12 Ω•m. The uncertainty on the depth estimate is 35%, which is acceptable, and the resistivity of 12 Ω•m does fully agree with the true resistivity of 10 Ω•m. Note that this result is obtained after a fully automatic procedure, in which the data have been weighted with the in situ measured electromagnetic noise.

Even when using an inversion algorithm which cannot handle non-uniform uncertainties on the sounding data, the noise model (fig. 7a) should still be useful as it draws the border between valid data and noise data. Simply cut off data at delay times after which the data have reached the noise line. Taking this approach to the data results (model not shown) in a depth of about 180 m and a resistivity of the halfspace just below 5 Ω•m.

Inversion of Field Data

The sounding shown in fig. 8 is from a hydrogeological investigation in Denmark and is one of about 200 soundings in the area. After the interpretations of the soundings a pump test well was drilled just next to the sounding site, enabling a comparison between the inversion and the drilling results.

The noise is measured on the segment with the highest repetition frequency and thereafter extrapolated over the entire time range. For illustration the error bars on the data are shown. At late times the error on the sounding data is about 100% as it reaches the noise line. A four layer model is employed to fit the sounding data. The result of the inversion is shown along with the drilling. As can be seen the agreement between the drilling and the inversion result is good. Note especially the excellent match between the low resistivity tertiary mica clay found at a depth of 144 in the drilling and the low resistivity layer found by the sounding at a depth of 149 m.

Conclusion

When white, Gaussian distributed electromagnetic noise is gated in intervals with lengths increasing with delay time and subsequently gate stacked, the mean noise is ideally proportional to $t^{-1/2}$. On log-log scale this corresponds to a linear noise model with a slope of -1/2. Through a numerical simulation of log-gating and gate stacking on white, Gaussian noise we have found that the slopes obtained show considerable scatter around this ideal slope.

An analysis of the characteristics of EM noise showed that the noise from a culturally disturbed area is not white and

in fact contains spectral peaks and a few outlier noise bursts. Nevertheless, noise models similar to those found in a numerical simulation of the white, Gaussian noise are obtained when measured EM series with an equidistant sampling are subjected to the log-gating, gate stacking process. Thus, we conclude that a linear noise model on log-log scale is valid for EM noise.

The noise model has been implemented as a mass production field procedure. Using the noise model the ambiguity of models is reduced as it becomes more obvious which part of the sounding curve is unreliable. Manual weeding out of data is shown to produce highly varying earth models, whereas use of the noise model to weight data according to the noise level produced a model in good agreement with the true model. Furthermore, a comparison of the model obtained from a noise weighted inversion of a TEM sounding with a nearby drillhole showed good correlation.

We have studied electromagnetic noise in culturally disturbed areas and present a way to take into account its effect on transient electromagnetic data. By in situ measurements of the electromagnetic noise, a noise model may be calculated and noise weighted data may be inverted to obtain a model of the electrical properties of the earth which better reflects the true resolution of the TEM method. The field work required is not increased and the subsequent processing is fully automatic.

Acknowledgments

We would like to thank Associate Prof. N. B. Christensen and Associate Prof. B. H. Jacobsen for fruitful discussions during the work. We are also grateful to Ph.D. K. I. Sorensen for providing us with the equidistantly sampled time series of the EM noise. Furthermore, we wish to thank an anonymous reviewer for critical comments which helped clarify the manuscript.

References

Auken, E., Christensen, N.B., Srensen, K.I., and Effers , F., 1994, Large scale hydrogeological investigation in the Beder area - A case study, Proc. Symp. on the Appl. of Geophys. to Engineering and Environmental Problems, Boston, 615-627.

Buselli, G., McCracken, K.G., and Thorburn, M., 1986, Transient electromagnetic response of the Teutonic Bore orebody, Geophysics, **51**, 957-963.

Christensen, N.B. and Auken, E., 1992, Simultaneous electromagnetic layered model analysis, In Proc. of the Interdisciplinary Inversion Workshop I, Jacobsen, B.H., Ed., GeoSkrifter, **41**, 49-56.

Fitterman, D.V., 1989, Detectability levels for central induction soundings, Geophysics **54**, 127-129.

Goldman, M., Gilad, D., Ronen, A. and Melloul, A., 1991, Mapping of seawater intrusion into the coastal aquifer of Israel by the time domain electromagnetic method, Geoexploration, **28**, 153-174.

Macnae, J.C., Lamontagne, Y. and West, G.F., 1984, Noise processing techniques for time-domain EM systems, Geophysics, **49**, 934-948.

McCracken, K.G., Oristalio, and Hohmann, G.W., 1986, Minimization of noise in electromagnetic exploration systems, Geophysics, **51**, 819-832.

Mills, T., Hoekstra, P., Blohm, M. and Evans, L., 1988, Time domain electromagnetic soundings for mapping seawater intrusion in Monterey, California, Ground Water, **26**, 771-782.

Nabighian, M.N., Macnae, J.C, 1991, Appendix A: TEM systems, In Electromagnetic methods in applied geophysics, Nabighian, M.N., Ed., II, 479-483.

Nekut, A.G. and Eaton, P.A., 1990, Effects of pipelines on EM soundings, 60th SEG meeting, 1990, Expanded Abstracts, 491-494.

Press, W.H., Teukolsky, S.A., Vetterling, W.T. and Flannery, B.P., 1992, Numerical recipes in Fortran, Cambridge University Press, 614 - 617.

Spies, B.R., 1989, Depth of investigation in electromagnetic sounding methods, Geophysics, **54**, 872-888.

Spies, B.R. and Frischkneckt, F.C., 1991, Electromagnetic sounding, In Electromagnetic methods in applied geophysics, Nabighian, M.N., Ed., II, 285-426.

Staples, P., 1984, Detection of massive sulphides beneath conductive overburden using the EM-37, Expl. Geophys., **15**, 33-36.

The use of tradenames is for descriptive purposes and does not imply endorsement by The Department of Earth Sciences, Geophysical Laboratory, Aarhus University.